

See discussions, stats, and author profiles for this publication at: <https://www.researchgate.net/publication/256773069>

Efficient 2.7 Micron Emission from Er³⁺/Pr³⁺ Codoped Oxyfluorotellurite Glass

ARTICLE *in* JOURNAL OF NON-CRYSTALLINE SOLIDS · DECEMBER 2012

Impact Factor: 1.77 · DOI: 10.1016/j.jnoncrysol.2012.08.016

CITATIONS

12

READS

38

6 AUTHORS, INCLUDING:



Gongxun Bai

The Hong Kong Polytechnic University

37 PUBLICATIONS 302 CITATIONS

SEE PROFILE



Yuen H. Tsang

The Hong Kong Polytechnic University

100 PUBLICATIONS 946 CITATIONS

SEE PROFILE



Efficient 2.7 micron emission from $\text{Er}^{3+}/\text{Pr}^{3+}$ codoped oxyfluorotellurite glass

Gongxun Bai ^a, Jia Ding ^b, Lili Tao ^a, Kefeng Li ^b, Lili Hu ^b, Yuen H. Tsang ^{a,*}

^a Department of Applied Physics and Materials Research Center, The Hong Kong Polytechnic University, Hong Kong, P.R. China

^b Key Laboratory of Materials for High Power Laser, Shanghai Institute of Optics and Fine Mechanics, Chinese Academy of Sciences, Shanghai 201800, P.R. China

ARTICLE INFO

Article history:

Received 12 July 2012

Received in revised form 21 August 2012

Available online xxxx

Keywords:

2.7 micron emission;
Oxyfluorotellurite glass;
Rare earths;
Er

ABSTRACT

2.7 μm emission from the Er^{3+} and $\text{Er}^{3+}/\text{Pr}^{3+}$ ions doped oxyfluorotellurite glasses was detected when pumped with a 980 nm laser diode and their results were compared. It is found that 2.7 μm emission from Er^{3+} is enhanced by codoped with Pr^{3+} in the oxyfluoride tellurite glass. The emission characteristic at 2.7 μm and energy transfer (ET) have been investigated. The fabricated glass possesses a larger calculated emission cross section ($1.01 \times 10^{-20} \text{ cm}^2$) along with a higher spontaneous transition probability (60.92 s^{-1}) corresponding to the $\text{Er}^{3+}: {}^4\text{I}_{11/2} \rightarrow {}^4\text{I}_{13/2}$ transition. Additionally, large ET efficiency of 85% indicates the more efficient ET process from Er^{3+} to Pr^{3+} ($\text{Er}^{3+}: {}^4\text{I}_{13/2} + \text{Pr}^{3+}: {}^3\text{H}_4 \rightarrow \text{Er}^{3+}: {}^4\text{I}_{15/2} + \text{Pr}^{3+}: {}^3\text{F}_3$). Therefore, codoping with Pr^{3+} ions can further improve the 2.7 μm emission of Er^{3+} via ET and the investigation of the materials in this study could help to find potential application of 2.7 μm laser.

© 2012 Elsevier B.V. All rights reserved.

1. Introduction

Due to the favourable thermal properties, high efficiency and potential applications in medical surgery, military countermeasures, atmosphere pollution monitoring, remote sensing and eye-safe laser radar [1–5], considerable attentions have recently been attracted to fiber lasers operating at $\sim 3 \mu\text{m}$ obtained from various rare earth lasing ions e.g. Dy^{3+} [2,3], Ho^{3+} [4], and Er^{3+} [5,6]. Er^{3+} ion is a particularly popular dopant for $\sim 3 \mu\text{m}$ generation because of the fact that its absorption peak ${}^4\text{I}_{15/2} \rightarrow {}^4\text{I}_{11/2}$ matches well with the emission waveband of the readily available low cost high power diode laser operating at near 980 nm. Therefore it is a popular way to obtain $\sim 3 \mu\text{m}$ from $\text{Er}^{3+}: {}^4\text{I}_{11/2} \rightarrow {}^4\text{I}_{13/2}$ transition when excited by a $\sim 980 \text{ nm}$ diode laser [5,6]. However, as the fluorescence lifetime of the upper-level, $\text{Er}^{3+}: {}^4\text{I}_{11/2}$ is considerably shorter than the lower-level [7], 2.7 μm luminescence cannot be acquired efficiently. To solve this problem, Cr^{3+} , Tm^{3+} , Ho^{3+} , Nd^{3+} , or Pr^{3+} is codoped with Er^{3+} ion as sensitizer ions to achieve population inversions of Er^{3+} ions for 2.7 μm emission [8–11].

Recent reports about Er^{3+} doped fiber lasers at 2.7 μm have mainly focused on fluoride glasses due to their low phonon energy and low optical attenuation at $3 \mu\text{m}$ in the typical water absorption band [12]. However, the stability and output power of fluoride fiber laser are limited by its low damage threshold, fragility and low thermal-shock resistance of fluoride glasses, not to mention its poor moisture resistance and manufacture difficulty. Therefore, tellurite glasses have drawn much interest owing to their combination of high transparency in middle infrared range, good thermal stability

and chemical durability, particularly their possession of a lower phonon energy amongst oxide glasses of $650\text{--}780 \text{ cm}^{-1}$ than phosphate, silicate, and germanate glasses, which leads to less multi-phonon relaxation rates as well as more efficient emission at 2.7 μm [13,14]. In addition, fluoride can be added to tellurite glasses and the formation of a local oxide and fluoride bonding environment around rare earth ions so as to reduce the OH^- group concentration and further minimise the background loss at the 2.7 μm [15]. In this paper, $\text{Er}^{3+}/\text{Pr}^{3+}$ codoped oxyfluoride tellurite glass proves to be a promising mid-infrared material for its practical application with the successful fabrication of $\text{Er}^{3+}/\text{Pr}^{3+}$ codoped oxyfluoride tellurite glass and the investigation of its 2.7 μm emission.

2. Experiments

2.1. Material synthesis

The glass samples were prepared with different compositions in mol. %. (1) TeO_2 (60–70%), ZnO (10–25%), Na_2O (5–10%), La_2O_3 (5–10%), named TZ; (2) TeO_2 (60–70%), ZnO (0–15%), ZnF_2 (10–15%), Na_2O (5–10%), La_2O_3 (3–10%), Er_2O_3 (x%), PrF_3 (y%), named TZF, $x=0,1$; $y=0,0.2$. Well mixed batches of 15 g were melted in a covered Pt–Au crucible at 900°C for 30 minutes. Then the melts were poured onto preheated brass mold, followed by annealing at 350°C for 2 hours. Finally, the formed samples were cut and optically polished to the thickness of 2 mm for the spectroscopic measurements.

2.2. Measurements

The glass density was measured by the Archimede's method using distilled water as the immersion fluid. The refractive index of host

* Corresponding author. Tel.: +852 27665676; fax: +852 23337629.

E-mail address: Yuen.Tsang@polyu.edu.hk (Y.H. Tsang).

glass was measured by Metricon Model 2010/M Prism Coupler. Mid-infrared transmittance spectra were recorded by a Perkin-Elmer 1600 series Fourier transform infrared (FTIR) spectrometer in the range of 1250 to 4000 cm^{-1} . Absorption spectra were measured with a Perkin-Elmer Lambda 900 UV/VIS/NIR spectrophotometer in the range of 400 to 2200 nm. Under the excitation of a 980 nm diode laser, upconversion, 1.5 μm , and 2.7 μm emissions as well as the lifetime of $\text{Er}^{3+}:^4\text{I}_{13/2}$ level were measured with an Edinburgh FLSP920 spectrophotometer. All the measurements were carried out at room temperature.

3. Results

3.1. Infrared transmittance

Fig. 1 illustrates mid-infrared transmission spectra of glasses with different fluoride concentration. TZF consists of 10 mol. % ZnF_2 , while TZ contains no fluoride. Both samples show good mid-infrared transmission near 2.7 μm , with ~80%, the 20% loss includes absorption, Fresnel reflections and dispersion of the glasses.

3.2. Absorption spectroscopy

Fig. 2 describes the absorption spectra of Er^{3+} singly doped and $\text{Er}^{3+}/\text{Pr}^{3+}$ codoped TZF samples in the range of 400 to 2200 nm at room temperature, and the absorption bands of Er^{3+} and Pr^{3+} corresponding to the transitions labelled starting from the ground state to the higher levels. The strong absorption around 980 nm suggests that this glass can be pumped efficiently with a 980 nm laser diode.

3.3. Fluorescence spectra

The infrared photoluminescence spectra of Er^{3+} singly doped and $\text{Er}^{3+}/\text{Pr}^{3+}$ codoped oxyfluorotellurite glasses were measured as shown in Fig. 3. Fig. 4 (a) shows the visible upconversion fluorescence spectra of oxyfluorotellurite glasses under 980 nm excitation.

4. Discussion

4.1. Infrared transmittance

The stretching vibration of free OH^- groups results in the absorption band ranging from 2.75 μm to 4.0 μm . It is obvious that fluoride is

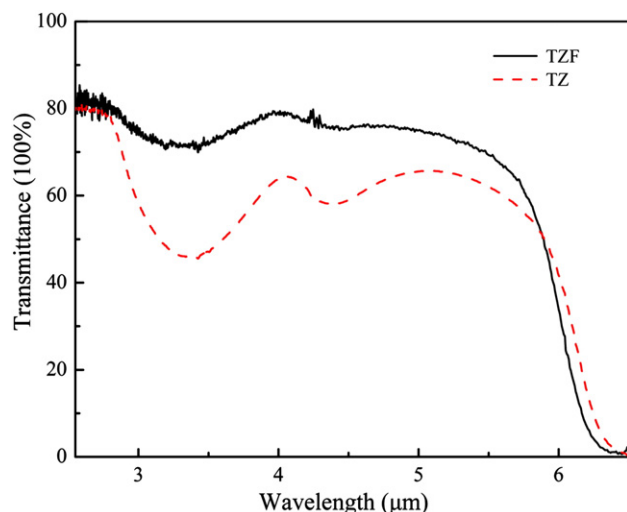


Fig. 1. Mid-infrared transmittance spectra of samples with different fluoride concentration. TZF consists of 10 mol. % ZnF_2 , while TZ contains no fluoride.

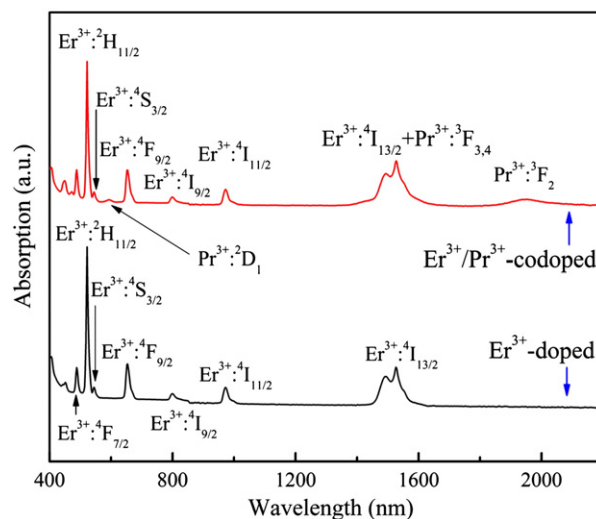


Fig. 2. Absorption spectra of prepared oxyfluorotellurite glass.

a highly efficient hydroxyl removal material in tellurite glasses through the reaction $\text{OH}^- + \text{F}^- \rightarrow \text{O}^{2-} + \text{HF}\uparrow$ [16]. It is well known that the concentration of OH^- group greatly affects mid-infrared emission efficiency of rare earth ions because the participation of the residual hydroxyl in the energy transfer (ET) of rare earth ions will give rise to the decrease in the emission. The content of hydroxyl can be defined by the absorption coefficient of OH^- vibration band around 3 μm , as described in [17]

$$\alpha_{\text{OH}^-} = l^{-1} \ln(T_0/T), \quad (1)$$

where l is the thickness of samples which is 2 mm and T_0 and T are the transmitted and incident intensities, respectively. Adding fluoride can decrease the absorption coefficient, α_{OH^-} around 3 μm from 2.77 cm^{-1} to 0.45 cm^{-1} , resulting in the dramatic improvement of the mid-infrared transmittance which makes the fabricated oxyfluoride tellurite a promising candidate for mid-infrared laser materials.

4.2. Judd–Ofelt analysis

From the absorption spectrum shown in Fig. 2, the experimental oscillator strength (f_{exp}) of the transitions can be calculated by using the following equation [14]

$$f_{\text{exp}} = \frac{2.303mc^2}{\pi e^2 Nd\lambda^2} \int \text{OD}(\lambda) d\lambda, \quad (2)$$

where m and e are the mass and charge of electron, c is the speed of the light in vacuum, N is the concentration of rare earth ions, $\int \text{OD}(\lambda) d\lambda$ is the integrated absorption coefficient, d is the sample thickness.

According to the Judd–Ofelt theory [18,19], the theoretical oscillator strength of an electric dipole transition from initial state $|S, L, J\rangle$ to an excited state $|S', L', J'\rangle$ can be expressed by

$$f_{\text{theor}}^{\text{ED}} = \frac{8\pi^2 m\nu}{3h(2J+1)} \left[\frac{(n^2+2)^2}{9n} \right] \times \sum_{t=2,4,6} \Omega_t |\langle S, L, J | U^\lambda | S', L', J' \rangle|^2, \quad (3)$$

where J is the total angular momentum for the ground state, ν is the transition frequency, $|U^\lambda|$ is the reduced matrix element, which is insensitive to the host environment, n is the refractive index. The refractive index n_d (587.6 nm) of TZF glass is 1.95. Ω_t ($t=2, 4, 6$) are the J–O intensity parameters. The Ω_t ($t=2, 4, 6$) parameters are calculated from

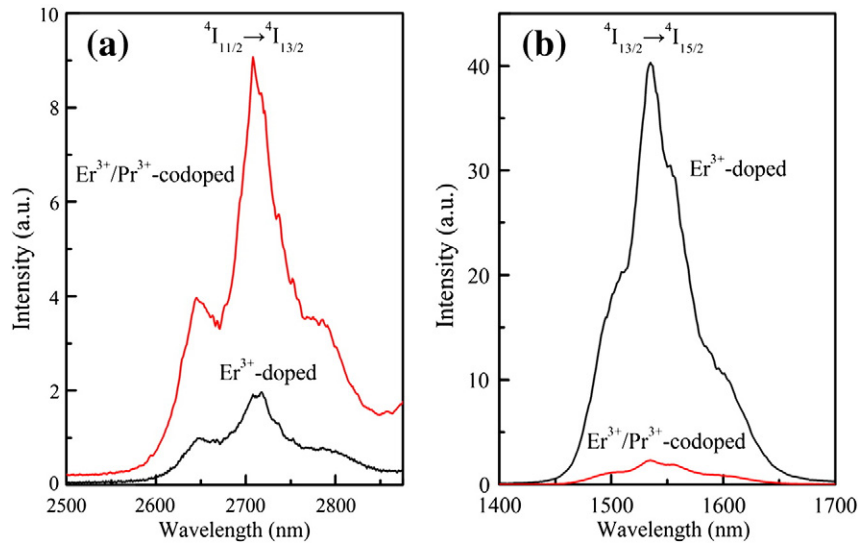


Fig. 3. (a) 2.7 μm and (b) 1.5 μm emission spectra of Er^{3+} singly doped and $\text{Er}^{3+}/\text{Pr}^{3+}$ codoped oxyfluorotellurite glasses pumped at 980 nm.

the measured values of oscillator strength for different transitions by using the least square fitting procedure. Theoretically, Ω_2 is strongly dependent on the local environment of rare earth ions sites and proportional to the covalence of $\text{Er}^{3+}-\text{O}^{2-}$, while Ω_6 is associated with the ionic bonding between Er^{3+} and coordinated anions. The calculated results show that $\Omega_2 = (5.4 \pm 0.17) \times 10^{-20} \text{ cm}^2$, $\Omega_4 = (2 \pm 0.09) \times 10^{-20} \text{ cm}^2$ and $\Omega_6 = (1.35 \pm 0.05) \times 10^{-20} \text{ cm}^2$ for Er^{3+} in our fabricated glass, the root-mean-square error deviation of intensity parameters is 0.31×10^{-6} , indicating the reliability of the calculation process. The Ω_2 of TZF is higher than that of LiYF_4 [20], fluoride [21] and fluorophosphates [11] glasses, showing that TZF glass possesses weaker covalence than those materials.

The radiative transition probabilities for the excited levels of Er^{3+} can be calculated by using the J–O parameters. The transition probabilities is given by [14]

$$A[(S, L)J; (S', L')J'] = A_{\text{ed}} + A_{\text{md}} = \frac{64\pi^4 e^2}{3h\lambda^3 (2J+1)} \times \left[\frac{n(n^2+2)^2}{9} S_{\text{ed}} + n^3 S_{\text{md}} \right], \quad (4)$$

where $\frac{n(n^2+2)^2}{9}$ is the local field correction for electric dipole transitions S_{ed} and n^3 for magnetic transitions S_{md} . S_{md} can be described by

$$S_{\text{md}} = \left(\frac{\hbar}{2mc} \right)^2 |\langle S, L, J || L + 2S || S', L', J' \rangle|^2, \quad (5)$$

The $|\langle S, L, J || L + 2S || S', L', J' \rangle|^2$ is nonzero only if $\Delta S = \Delta L = 0$, $\Delta J = 0, \pm 1$. The radiative lifetime is related to radiative transitions probabilities by

$$\tau_{\text{rad}} = \left\{ \sum_{S', L', J'} A[(S, L)J; (S', L')J'] \right\}^{-1}, \quad (6)$$

The fluorescence branching ratio can be obtained from the transition probabilities by using

$$\beta_{J'} = \beta[(S, L)J; (S', L')J'] = \frac{A[(S, L)J; (S', L')J']}{\sum_{S', L', J'} A[(S, L)J; (S', L')J']} \quad (7)$$

The branching ratio and spontaneous transition probabilities of the Er^{3+} : ${}^4\text{I}_{11/2} \rightarrow {}^4\text{I}_{13/2}$ transition are 16% and 60.92 s^{-1} , respectively,

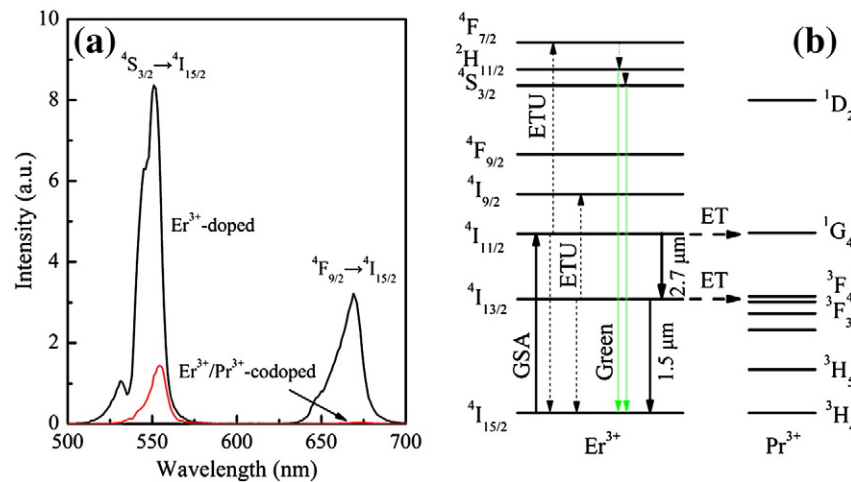


Fig. 4. (a) Upconversion fluorescence spectra of Er^{3+} singly doped and $\text{Er}^{3+}/\text{Pr}^{3+}$ codoped oxyfluorotellurite glass. (b) Energy transfer sketch of $\text{Er}^{3+}/\text{Pr}^{3+}$ codoped oxyfluorotellurite glass pumped at 980 nm.

which are both higher than the results of fluoride (14.1% and 13 s^{-1}) [21] and germanate (14.4% and 47.8 s^{-1}) [22] glasses, since the radiative transition probability depends intensively on the refractive index, it is reasonable to obtain large A_{rad} in tellurite glass, and the high value is beneficial in achieving intense $2.7 \mu\text{m}$ emission.

4.3. Fluorescence spectra and mechanism analysis

Fig. 3 shows that the emission intensity at $2.7 \mu\text{m}$ from $\text{Er}^{3+}/\text{Pr}^{3+}$ codoped oxyfluorotellurite glass is quite strong, whereas $1.5 \mu\text{m}$ emission is almost absent. Intense $2.7 \mu\text{m}$ emission in $\text{Er}^{3+}/\text{Pr}^{3+}$ codoped glass is mainly due to ET between $\text{Er}^{3+}: {}^4\text{I}_{13/2}$ and $\text{Pr}^{3+}: {}^3\text{F}_{3,4}$. A significant reduction in the emission intensity of $1.5 \mu\text{m}$ is detected between Er^{3+} singly doped and $\text{Er}^{3+}/\text{Pr}^{3+}$ codoped glasses, and the lifetime of $\text{Er}^{3+}: {}^4\text{I}_{13/2}$ level was reduced from 2.84 ms to 0.43 ms. It is deduced that Pr^{3+} ions can be used effectively to depopulate $\text{Er}^{3+}: {}^4\text{I}_{13/2}$. According to the emission spectra and Fuchtbauer–Ladenburg theory, the $2.7 \mu\text{m}$ emission cross section, σ_{e} , can be calculated by

$$\sigma_{\text{em}}(\lambda) = \frac{\lambda^5}{8\pi c n^2 \tau_{\text{rad}}} \cdot \frac{I(\lambda)}{\int \lambda I(\lambda) d\lambda} \quad (8)$$

where τ_{rad} is the effective lifetime of the spontaneous radiation, n is the refractive index, c is the velocity of light and λ is the wavelength. It is noteworthy that the maximum of the calculated emission cross section in $\text{Er}^{3+}/\text{Pr}^{3+}$ codoped oxyfluorotellurite glass achieves $1.01 \times 10^{-20} \text{ cm}^2$ at $2.7 \mu\text{m}$, which is larger than the results of Er^{3+} doped ZBLAN glass ($5.7 \times 10^{-21} \text{ cm}^2$) [23], $\text{Er}^{3+}/\text{Pr}^{3+}$ codoped germanate glass ($7.02 \times 10^{-21} \text{ cm}^2$) [17] and fluorophosphates glass ($6.57 \times 10^{-21} \text{ cm}^2$) [11]. It indicates that fabricated glass with excellent properties has potential application in high-power $2.7 \mu\text{m}$ laser.

Fig. 4 shows the intensity of green emission signal decreases drastically, and the red emission signal even disappears when codoping with Pr^{3+} ions. Energy level figure of Er^{3+} and Pr^{3+} ions evaluates the processes of ground state absorption (GSA), energy transfer (ET), energy transfer upconversion (ETU). It is noted that ET process ($\text{Er}^{3+}: {}^4\text{I}_{13/2} + \text{Pr}^{3+}: {}^3\text{H}_4 \rightarrow \text{Er}^{3+}: {}^4\text{I}_{15/2} + \text{Pr}^{3+}: {}^3\text{F}_3$) is much more efficient than that of ($\text{Er}^{3+}: {}^4\text{I}_{11/2} + \text{Pr}^{3+}: {}^3\text{H}_4 \rightarrow \text{Er}^{3+}: {}^4\text{I}_{15/2} + \text{Pr}^{3+}: {}^1\text{G}_4$), because the oscillator strength of the former ET is extremely larger than the latter. The efficiency of ET process can be calculated by using the lifetime values with the following equation [24]:

$$\eta_{\text{ET}} = 1 - \frac{\tau_{\text{Er/Pr}}}{\tau_{\text{Er}}} \quad (9)$$

Where $\tau_{\text{Er/Pr}}$ and τ_{Er} are the lifetimes of $\text{Er}^{3+}: {}^4\text{I}_{13/2}$ level were measured at $1.5 \mu\text{m}$, with and without Pr^{3+} ions, respectively. The value of η_{ET} from ($\text{Er}^{3+}: {}^4\text{I}_{13/2} + \text{Pr}^{3+}: {}^3\text{H}_4 \rightarrow \text{Er}^{3+}: {}^4\text{I}_{15/2} + \text{Pr}^{3+}: {}^3\text{F}_3$)

is up to 85% for $\text{Er}^{3+}/\text{Pr}^{3+}$ codoped oxyfluorotellurite glass. Therefore, Pr^{3+} ions can efficiently quench $\text{Er}^{3+}: {}^4\text{I}_{13/2}$ level by ET and enhance $2.7 \mu\text{m}$ emission.

5. Conclusions

In conclusion, enhanced $2.7 \mu\text{m}$ emission from $\text{Er}^{3+}/\text{Pr}^{3+}$ codoped oxyfluoride tellurite glass was observed when pumped with a 980 nm laser diode. The fabricated glass possesses a larger calculated emission cross section ($1.01 \times 10^{-20} \text{ cm}^2$) along with a higher spontaneous transition probability (60.92 s^{-1}) corresponding to the $\text{Er}^{3+}: {}^4\text{I}_{11/2} \rightarrow {}^4\text{I}_{13/2}$ transition. In addition, large ET efficiency of 85 % indicates that the ET process from Er^{3+} to Pr^{3+} ($\text{Er}^{3+}: {}^4\text{I}_{13/2} + \text{Pr}^{3+}: {}^3\text{H}_4 \rightarrow \text{Er}^{3+}: {}^4\text{I}_{15/2} + \text{Pr}^{3+}: {}^3\text{F}_3$) is efficient. The results explain why the enhancement of $2.7 \mu\text{m}$ emission can be achieved in this material and show that $\text{Er}^{3+}/\text{Pr}^{3+}$ codoped oxyfluorotellurite glass can potentially be used as an efficient gain media in the $2.7 \mu\text{m}$ fiber laser system.

Acknowledgments

The authors thank the support from The Hong Kong Polytechnic University (grants G-YH91, G-YJ20, and A-PK72), the research grants Council of Hong Kong, China, GRF 526511 (PolyU code: B-Q26E).

References

- [1] M.C. Pierce, S.D. Jackson, M.R. Dickinson, T.A. King, P. Sloan, *Lasers Surg. Med.* 26 (2000) 491.
- [2] Y.H. Tsang, A. El-Taher, T.A. King, S.D. Jackson, *Opt. Express* 14 (2006) 678.
- [3] Y.H. Tsang, A.E. El-Taher, *Laser Phys. Lett.* 8 (2011) 818.
- [4] F.Z. Qamar, T.A. King, S.D. Jackson, Y.H. Tsang, *IEEE J. Lightwave Technol.* 23 (2005) 4315.
- [5] X. Zhu, R. Jain, *Opt. Lett.* 32 (2007) 2381.
- [6] M. Pollnan, S.D. Jackson, *IEEE J. Sel. Top. Quantum Electron.* 7 (2001) 30.
- [7] X. Zhu, R. Jain, *Opt. Lett.* 33 (2008) 1578.
- [8] Y. Tian, R. Xu, L. Hu, J. Zhang, *J. Quant. Spectrosc. Radiat. Transfer* 113 (2011) 87.
- [9] L. Zhang, Z. Yang, Y. Tian, J. Zhang, L. Hu, *J. Appl. Phys.* 110 (2011) 093106.
- [10] Y. Guo, M. Li, Y. Tian, R. Xu, L. Hu, J. Zhang, *J. Appl. Phys.* 110 (2011) 013512.
- [11] Y. Tian, R. Xu, L. Zhang, L. Hu, J. Zhang, *Opt. Lett.* 36 (2011) 109.
- [12] X. Zhu, R. Jain, *Opt. Lett.* 32 (2007) 26.
- [13] B. Richards, A. Jha, Y. Tsang, D. Binks, J. Lousteau, F. Fusari, A. Lagatsky, C. Brown, W. Sibbett, *Laser Phys. Lett.* 7 (2010) 177.
- [14] K. Li, Q. Zhang, G. Bai, S. Fan, J. Zhang, L. Hu, *J. Alloys Compd.* 504 (2010) 573.
- [15] G. Gao, G. Wang, C. Yu, J. Zhang, L. Hu, *J. Lumin.* 129 (2009) 1042.
- [16] A. Lin, A. Ryasnyanskiy, J. Toulouse, *Opt. Lett.* 36 (2011) 740.
- [17] R. Xu, Y. Tian, L. Hu, J. Zhang, *Opt. Lett.* 36 (2011) 1173.
- [18] B.R. Judd, *Phys. Rev.* 127 (1962) 750.
- [19] G.S. Ofelt, *J. Chem. Phys.* 37 (1962) 511.
- [20] S. Hubert, D. Meichenin, B. Zhou, F. Auzel, *J. Lumin.* 50 (1991) 7.
- [21] A. Florez, Y. Messaddeq, O.L. Malta, M.A. Aegerter, *J. Alloys Compd.* 227 (1995) 135.
- [22] R. Balda, A. Oleaga, J. Fernandez, J. Fdez-Navarro, *Opt. Mater.* 24 (2003) 83.
- [23] S.D. Jackson, T.A. King, M. Pollnau, *J. Mod. Opt.* 47 (2000) 1987.
- [24] J. Heo, W.Y. Cho, W.J. Chung, *J. Non-Cryst. Solids* 212 (1997) 151.